Universiteit
Leiden
The Netherlands

Tracking helminths : from molecular diagnostics to mechanisms behind immune polarization

Kaisar, M.M.

Citation
Kaisar, M. M. (2017, September 19). *Tracking helminths : from molecular diagnostics to mechanisms behind immune polarization*. Retrieved from https://hdl.handle.net/1887/57928

Version:	Not Applicable (or Unknown)
License:	Licence agreement concerning inclusion of doctoral thesis in the Institutional Repository of the University of Leiden
Downloaded from:	https://hdl.handle.net/1887/57928

Note: To cite this publication please use the final published version (if applicable).

Cover Page

Universiteit Leiden

The handle http://hdl.handle.net/1887/57928 holds various files of this Leiden University dissertation

Author: Kaisar, M.M.
Title: Tracking helminths : from molecular diagnostics to mechanisms behind immune polarization
Issue Date: 2017-09-19

Chapter 5

Human dendritic cells with Th2-polarizing capacity: analysis using label-free quantitative proteomics

MARIA M. M. KAISAR[1, 2, #], LEONIE HUSSAARTS[1, #], ARZU TUGCE GULER[3], HANS DALEBOUT[3], BART EVERTS[1], ANDRÉ M. DEELDER[3], MAGNUS PALMBLAD[3], MARIA YAZDANBAKHSH[1]

[1]Department of Parasitology, Leiden University Medical Center (LUMC), Leiden, The Netherlands
[2]Department of Parasitology, Faculty of Medicine, Universitas Indonesia, Jakarta, Indonesia
[3]Center of Proteomics and Metabolomics, LUMC, Leiden, The Netherlands
[#]Contributed equally

International Archives of Allergy and Immunology. 2017

ABSTRACT

Dendritic cells (DCs) are the sentinels of the immune system. Upon recognition of a pathogen, they mature and migrate to draining lymph nodes to prime and polarize T cell responses. Although it is known that helminths and helminth-derived molecules condition DCs to polarize T helper (Th) cells towards Th2, the underlying mechanisms remain incompletely understood. The aim of this study was to conduct a proteome analysis of helminth antigen-stimulated DCs, in order to gain more insight into the cellular processes associated with their ability to polarize immune responses. We analyzed maturation and polarization of monocyte-derived DCs from nine donors at two different time points after stimulation with different Th1 and Th2-polarizing pathogen-derived molecules. The samples were measured using liquid chromatography-Fourier transform ion cyclotron resonance mass spectrometry (LC-FTICRMS) for relative quantitation. Lipopolysaccharide (LPS)-induced maturation promoted expression of proteins related to metabolic, cellular and immune system processes. Th1 polarizing DCs, conditioned by IFN-γ during maturation, displayed accelerated maturation by differentially expressing cytoskeletal proteins and proteins involved in immune regulation. Stimulation of DCs with Souluble Egg Antigents (SEA) and omega-1 derived from *Schistosoma mansoni*, two Th2-inducing stimuli, increased 60S acidic ribosomal protein P2 (RPLP2) and vesicle amine transferase 1 (VAT1) while decreasing the expression of proteins related to antigen processing and presentation. Our data indicate that not only proteins involved in interaction between T cells and DCs at the level of the immunological synapse but also those related to cellular metabolism and stress may promote Th2 polarization.

Keyword:
Dendritic cells, Helminths, Omega-1, Proteome, T helper 2 responses

INTRODUCTION

Dendritic cells (DCs) [1] are professional antigen-presenting cells located in peripheral tissues, that continuously sample the environment to capture antigens from invading microbes. Upon recognition of pathogens-associated molecules, DCs undergo maturation and migrate to the draining lymph nodes where they present antigen to antigen-specific T helper (Th) cells. Different classes of pathogens polarize DCs for the induction of different types of Th cell responses. In general, rapidly replicating intracellular microorganisms such as viruses and certain bacteria promote the differentiation of Th1 cells. The principal regulators of anti-helminth immunity are Th2 cells, and fungi and extracellular bacteria drive Th17 responses [2-4].

While much is known about the regulation of Th1 and Th17 responses, the mechanisms that control Th2 activation are still not fully understood [5]. Although helminths are strong inducers of Th2 responses, it has proven to be difficult to pinpoint the specific mechanisms involved due to the complex nature of many helminth-derived antigen preparations. For example, *Schistosoma mansoni* soluble egg antigen (SEA), among the most widely used preparations for studying immune responses to helminth antigens, contains more than 600 different proteins [6]. The identification of omega-1 as a major immunomodulatory component in SEA therefore provided an opportunity to further dissect the molecular mechanisms underlying Th2 skewing [7, 8]. We have previously shown that omega-1 (ω-1) is a glycosylated T2 RNase that conditions DCs for Th2 induction by suppressing protein synthesis [9]. However, it remains unclear which mechanisms subsequently enable Th2 skewing.

Maturation of DCs is characterized by changes in expression of a large number of proteins [10]. Therefore, as a representative indicator of cell function and phenotype, various groups have studied the proteome of pro-Th2 DCs. Using semi-quantitative gel-based techniques, three cytoplasmic proteins were found to be exclusive to the Th2-inducing proteome of human monocyte-derived DCs [11]. In mouse bone marrow-derived DCs (BMDCs), four proteins were significantly affected by stimulation with helminth antigens [12]. A third study on pro-Th2 BMDCs used iTRAQ labeling for relative quantitation of plasma membrane proteins, and showed that pro-Th2 BMDCs upregulated proteins related to cell metabolism and downregulated proteins associated with the cytoskeleton [13]. Although these studies provide valuable directions for future research, the use of 2-DE and iTRAQ does not allow for high-throughput analysis and direct comparison of a large number of biological replicates. This is especially relevant when donor-to-donor variation is expected, for example when working with DCs from human donors, and may explain why only very few proteins were found in common between different gel-based studies on lipopolysaccharide (LPS)-matured human DCs [10, 11, 14, 15].

As such, the introduction of a high-resolution label-free and gel-free method for quantitative analysis of DC proteomes would be highly beneficial. In this study, we analyzed DC maturation and polarization using liquid chromatography fourier transform ion cyclotron resonance mass spectrometry (LC-FTICRMS) for accurate mass measurement and relative quantitation [16, 17]. This method allowed us to include a total of nine DC donors and four different stimuli. We included an early (6 h) and a late (32 h) time point in addition to baseline (0 h), to reflect maturation stages associated with migration and antigen presentation. This experimental set-up enabled us to take in donor-to-donor variation in the global proteome into consideration and quantify the most abundant proteins across a large number of replicates. Using SEA, a complex antigen preparation, and ω-1, a single molecule for Th2 polarization, we here focused on the identification of proteins associated with the pro-Th2 DC proteome.

MATERIAL AND METHODS

Human DC culture, stimulation, and analysis

Monocytes isolated from venous blood of 9 healthy volunteers were differentiated as described previously [18]. On day 6 the immature DCs (iDCs) were stimulated with SEA (50 µg/mL), ω-1 (250 ng/mL) or IFN-γ (1000 U/mL) in the presence of 100 ng/mL ultrapure LPS (*E. coli* 0111 B4 strain, InvivoGen) and human rGM-CSF (20 ng/ml; Life Technologies). At the indicated time points, samples were collected for protein extraction and digestion as described below. Alternatively, after 48 h of stimulation, expression of surface molecules was determined by flow cytometry (FACSCanto, BD Biosciences) using the following antibodies: CD14 PerCP, CD86 FITC (both BD Biosciences), and CD1a PE (Beckman-Coulter). In addition, $1x10^4$ 48 h-matured DCs were co-cultured with $1x10^4$ CD40L-expressing J558 cells. Supernatants were collected after 24 h and IL-12p70 concentrations were determined by ELISA using mouse anti-human IL-12 (clone 20C2) as a capture antibody and biotinylated mouse anti-human IL-12 (clone C8.6) as a detection antibody (BD Biosciences). Volunteers signed informed consent forms and the samples were handled according to the guidelines described by the Dutch Federation of Medical Scientific Societies in the Code of Conduct for the responsible use of human tissue for medical research. Available from URL: www.fedra.org (accessed on September 2013).

Human T cell culture and analysis of T cell polarization

For analysis of T cell polarization, $5x10^3$ matured DCs were cultured with $2x10^4$ allogeneic naive $CD4^+$ T cells that were isolated from buffy coat (Sanquin) peripheral blood mononuclear cells using a $CD4^+/45RO^-$ Naive T Cell Enrichment Column (R&D Systems). Co-cultures were performed in the presence of staphylococcal enterotoxin B (10 pg/mL). On days 6 and 8, rhuIL-2 (10 U/mL, R&D Systems) was added and the T cells were expanded until day 11. Intracellular cytokine production was analyzed after restimulation with 100 ng/mL phorbol myristate acetate plus 1 µg/mL ionomycin for 6 h; 10 µg/mL brefeldin A was added during the last 4 h and the cells were fixed with 3.7% paraformaldehyde (all Sigma-Aldrich). The cells were permeabilized with 0.5% saponin (Sigma-Aldrich) and stained with PE- and FITC-labelled antibodies against IL-4 and IFN-γ, respectively (BD Biosciences).

Protein extraction and in-solution digestion

Cells were harvested with PBS at the indicated time points and centrifuged at 522×*g* for 8 minutes at 4 °C, after which they were transferred with 1 mL PBS to a micro centrifuge tube and centrifuged for 5 minutes at 5000 ×*g,* 4 °C. The supernatant was removed and pellets were snap-frozen in liquid nitrogen and stored at -80 °C. Samples were thawed in 30 µL lysis buffer consisting of 1% SDS, 125 U/mL benzonase nuclease (Sigma), 2 mM MgCl2, and protease inhibitors (complete ULTRA tablets, mini, EDTA-free, Roche) in 50 mM ammonium biocarbonate (ABC). Samples were placed at 95 °C for 5 min and following centrifugation at 16000 ×*g* for 30 min, the supernatant was collected. A BCA assay (Pierce Biotechnology) was conducted to determine the protein concentration. An equivalent of 10 µg protein was dissolved in 25 µL ABC and reduced using 10 mM DTT (Sigma) for 5 min at 95 °C, followed by 1 h alkylation using 40 mM iodoacetamide (Sigma) at room temperature. Using 3 kDa spin filters, the remainder of the lysis buffer was exchanged for ABC according to manufacturer's protocol (Millipore), and samples were digested for 17 h with sequencing-grade trypsin (Promega) at an enzyme to protein ratio of 1:50. The

digestion was quenched with 2% trifluoracetic acid to lower the pH. Peptide samples were stored at -35 °C until analysis.

Liquid chromatography - mass spectrometry

Accurate mass tags (AMTs) analysis was used to normalize the chromatograms for peptides and proteins identification across different stimulations and between different donors [19]. All samples were analyzed using a splitless NanoLC-Ultra 2D plus (Eksigent) system for parallel liquid chromatography (LC) with additional trap columns for desalting. The LC systems were configured with 300 µm-i.d. 5-mm PepMap C18 trap columns (Thermo Fisher Scientific) and 15-cm 300 µm-i.d. ChromXP C18 columns (Eksigent). Peptides were separated by a 90-minute linear gradient from 4 to 33% acetonitrile in 0.05% formic acid with the 4 µl/min flow rate. The LC systems were coupled on-line to amaZon speed ETD high-capacity 3D ion traps and a 12 T solariX FTICR system (all from Bruker Daltonics) in an FTICR-ion trap cluster [17]. For peptide identification in the ion traps, we generated three sample pools. Pool 1 contained a fraction of each sample that was stimulated for 32 h with LPS or LPS + IFN-γ. Pool 2 contained a fraction of each 0 h and 6 h iDC sample. Pool 3 contained a fraction of each uneven sample (all samples received a random number). These sample pools were run in triplicate on the ion traps. Up to ten abundant multiply charged precursors in m/z 300-1300 were selected for MS/MS in each MS scan in a data-dependent manner. After having been selected twice, each precursor was excluded for one minute. The LC systems were controlled using the HyStar 3.4 (Bruker) with a plug-in from Eksigent, the amaZon ion trap by trapControl 7.0, and the solariX FTICR system by solariXcontrol 1.3 (both Bruker).

Data analysis

The raw datasets from ion trap LC-MS/MS and LC-FTICRMS were converted to mzXML (48). The mzXML files were analysed using a scientific workflow called "Label-free proteomics using LC-MS" (http://www.myexperiment.org/workflows/4552.html). The workflow was designed using the Taverna workflow management system [20].

The LC-MS/MS data was used for identification. The TANDEM application [21] from the X! Tandem provided in Trans Proteomics Pipeline V4.7.7 was run to match the spectra with tryptic peptide sequences derived from UniProt *Homo sapiens* reference proteome database retrieved on 25.07.2014, for each pooled sample. The k-score plug-in was selected for the search with a minimum ion count of 1, and 2 maximum missed cleavage sites. The allowed parent monoisotopic mass error was ±5.0 Da, and the allowed fragment monoisotopic mass error was 0.4 Da. After peptide assignments to MS/MS spectra, the results were converted to pepXML format, an XML-based format that is used in peptide-level analysis [22], using the Tandem2XML application.

To use the high-resolution MS profiles for more precise quantification, each pepXML file was aligned with one master LC-FTICRMS data file. The alignment was done with pepAlign [23], which uses a genetic algorithm to align the two chromatographic time scales with a partial linear function. The output from pepAlign was the breakpoints of this function. The alignment was based on the X! Tandem expect scores and allowed a mass measurement error of ±50 ppm. The retention times in each pepXML file were changed according to the chromatographic alignment function by the pepWarp program. The accuracy of the peptide assignments to tandem mass spectra was assessed by PeptideProphet using the xinteract application provided in Trans Proteomics Pipeline V4.6.3 [24]. This application also combined the input datasets, so that all

identifications with assigned probabilities were contained in a single output file. This validated pepXML was then aligned with each individual LC-FTICRMS dataset. For quantitation of identified peptides, we used only peptides with PeptideProphet probabilities higher than 0.9369, giving a peptide-spectrum match false discovery rate of 1.0%. Modified peptides were not included.

The monoisotopic mass was calculated for each peptide of interest and the maximum intensity corresponding to this mass was extracted from a window ±60 seconds relative to the aligned retention time and ±25 ppm relative to the calculated mass. As the final output of the workflow, all peptide quantifications were combined into a single table where each row represents a peptide sequence and each column contains the intensity of that peptide in each sample. Missing values were imputed from a normal distribution representing the background signal removed during acquisition. A final matrix was created with proteins identified by more than two peptides, where the abundance of each protein was calculated as the median intensity of its peptides and normalized to the total signal intensity of all proteins in the entire LC-MS dataset. Fold changes in protein abundance between conditions were calculated in R based on the mean fold change of the nine different donors, and corresponding p-values were obtained from paired Student's t-testing of log-transformed protein intensities for each treatment and time point.

The heat-map for visualizing the regulated proteins of differently stimulated moDCs was generated using GENE-E software from the Broad Institute (https://software.broadinstitute.org/GENE-E/). Statistical analysis and visualization of differentially expressed proteins was performed using GraphPad Prism version 6.00 (GraphPad Software, La Jolla, CA USA) for Windows.

RESULTS

Functional characterization of human DCs

Immature DCs (iDCs) generated from nine donors were stimulated LPS in combination with IFN-γ as a Th1-inducing stimulus, and SEA or ω-1 as Th2-inducing conditions. The purpose of co-stimulation with LPS was to achieve a similar level of activation among the differently T polarizing DCs, to prevent the possibility that potential differences in activation status of the differently

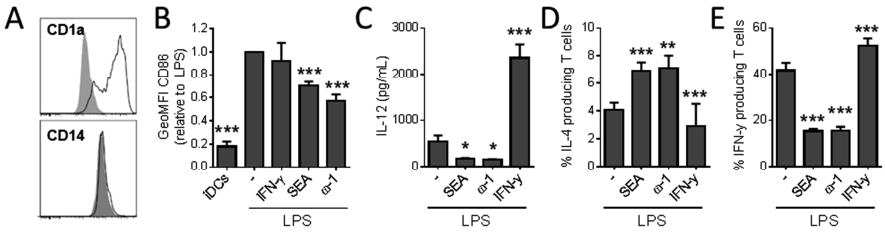

Figure 1. Functional characterization of pro-Th1 and pro-Th2 DCs

Monocyte-derived DCs were either left untreated or pulsed with LPS in the presence or absence of IFN-γ, SEA, or ω-1. After 48 h, expression of surface markers was analyzed by flow cytometry. (A) Representative histograms for expression of CD1a and CD14 are shown. (B) Expression levels of CD86, based on the geometric mean fluorescence, are shown relative to LPS, which was set to 1. (C) Following stimulation, moDCs were co-cultured with a CD40L-expressing cell line. Supernatants were collected after 24 h and IL-12p70 concentrations were determined by ELISA. (D) 48 h-matured DCs were cultured with allogeneic naive $CD4^+$ T cells for 11 days. Intracellular cytokine production as analyzed by flow cytometry after 6 h of stimulation with phorbol myristate acetate and ionomycin. The percentages of T cells uniquely positive for either IL-4 or (E) IFN-γ are shown. Box and whiskars ; *P<0.05; **P<0.01; ***<0.001 for significant differences with the LPS control based on a paired Student's t-test.

polarizing DCs would affect their T cell-polarizing characteristics. To functionally characterize these DCs, a co-culture system of human matured DCs and allogeneic naive $CD4^+$ T cells was used. Efficient differentiation of monocytes towards DCs was validated by expression high levels of CD1a and little CD14 (Figure 1A) and upregulation of CD86 expression upon LPS stimulation (Figure 1B). Additional stimulation with IFN-γ did not affect LPS-induced CD86 expression but strongly induced IL-12p70 production (Figure 1C), while SEA and ω-1 decreased expression of both CD86 and IL-12p70, as described previously (9). Analysis of T cell cytokine production confirmed that ω-1 and SEA induced a Th2 response, characterized by a high frequency of IL-4-producing T cells (Figure 1D), while stimulation of DCs with IFN-γ promoted a Th1 response (Figure 1E).

Protein Identifications

To establish the effect of maturation and polarization on the DC proteome, iDCs and LPS-matured DCs stimulated with IFN-γ, SEA or ω-1, were collected from each of the nine donors at three different time points: before stimulation (0 h), 6 hours after stimulation (6 h) and 32 h after stimulation (32 h). Proteins were digested after which peptides were identified using LC-MS/MS in an ion trap, resulting in the identification of 1159 unique peptides from 439 unique proteins with a false-discovery rate (FDR) of 1.0%. These were used for matching with and querying the LC-FTICRMS data for label-free quantitation [16, 17]. In total, 208 proteins corresponding to the most abundantly present proteins in these cells were quantified with multiple peptides in each biological replicate and at each time point. For analysis purposes we exclude one protein with the accession code Q9BZQ8 as the signal indicates that this protein was attributed to the VLTSEDEYNLLSDR peptide in NIBAN which is likely to come from the $^{13}C_1$-peak of the YCLQLYDETYER peptide from SEA-derived protein interleukin-4-inducing protein (IPSE). IPSE is known to be one of the most abundant proteins in SEA but has no Th2 polarizing activity [7], therefore irrelevant as a DC protein that constitutes pro-Th2 proteomes.

Effects of maturation on the human DC proteome

To identify proteins that were differentially expressed between the different stimulations, the stimulus-induced fold change in abundance was determined for each protein, by calculating the mean fold change of the nine donors. Corresponding *p*-values were obtained from a paired Student's t-test after log-transformation. Proteins were considered differentially expressed when $p<0.05$ and the stimulus induced fold change was more than 1.5-fold decreased or increased (i.e. fold change <0.67 or >1.5). LPS-induced maturation displayed a pronounced effect on the DC proteome. Compared to iDCs, LPS promoted differential expression of 10 proteins after 6 h (Table 1). Analysis of protein classification according to Gene Ontology terms indicated that the 8 upregulated proteins are mostly involved in transport or cell communication. The two downregulated proteins were both cytoskeletal proteins. After 32 h, LPS promoted differential expression of 22 proteins (Table 1). The majority of proteins was upregulated and related to different metabolic, cellular and immune system processes or transport. The protein most strongly upregulated by LPS stimulation was TNF receptor-associated factor 1 (TRAF1), an adapter molecule that regulates activation of NF-κB and JNK [25]. In addition, actin cross-linking proteins Fascin and Myristoylated alanine-rich C-kinase substrate (MARCS) were profoundly induced, as well as the MHC class I molecule HLA-B, involved in antigen presentation. Among the four downregulated proteins we identified Macrophage mannose receptor 1, that is involved in antigen uptake,

Table 1. Differentially expressed proteins in LPS-DCs versus iDCs

Accession	Protein	6 hours		32 hours	
		Fold	*p*-value	Fold	*p*-value
LPS-modulated, 6 hours					
P45880	Voltage-dependent anion-selective channel protein 2	2,74E+00	**4,40E-02**	1,81E+00	5,65E-01
P30040	Endoplasmic reticulum resident protein 29	2,59E+00	**3,12E-03**	1,67E+00	6,36E-01
Q13077	TNF receptor-associated factor 1	2,25E+00	**8,42E-03**	1,49E+01	**3,32E-06**
P61604	10 kDa heat shock protein. mitochondrial	2,23E+00	**3,28E-02**	1,68E+00	7,58E-01
P05362	Intercellular adhesion molecule 1	1,89E+00	**6,60E-04**	3,60E+00	**6,99E-03**
P30464*	HLA class I histocompatibility antigen, B-15 alpha chain	1,83E+00	**2,50E-02**	7,89E+00	**7,06E-04**
P29966	Myristoylated alanine-rich C-kinase substrate	1,77E+00	**2,18E-02**	1,08E+01	**8,81E-06**
Q9BQE5	Apolipoprotein L2	1,64E+00	**4,92E-02**	2,95E+00	**2,05E-03**
Q71U36	Tubulin alpha-1A chain	6,29E-01	**3,38E-02**	1,58E+00	8,17E-01
P06396	Gelsolin	6,21E-01	**5,29E-04**	1,96E+00	4,75E-01
LPS- modulated, 32 hours					
Q13077	TNF receptor-associated factor 1	2,25E+00	**8,42E-03**	1,49E+01	**3,32E-06**
P29966	Myristoylated alanine-rich C-kinase substrate	1,77E+00	**2,18E-02**	1,08E+01	**8,81E-06**
P30464*	HLA class I histocompatibility antigen, B-15 alpha chain	1,83E+00	**2,50E-02**	7,89E+00	**7,06E-04**
Q16658	Fascin	1,26E+00	6,06E-01	5,48E+00	**1,68E-04**
P04179	Superoxide dismutase [Mn], mitochondrial	1,20E+00	6,78E-01	4,66E+00	**7,52E-04**
P23381	Tryptophan--tRNA ligase, cytoplasmic	9,83E-01	5,47E-01	3,77E+00	**6,27E-06**
Q9UL46	Proteasome activator complex subunit 2	9,17E-01	2,54E-01	3,68E+00	**6,65E-04**
P05362	Intercellular adhesion molecule 1	1,89E+00	**6,60E-04**	3,60E+00	**6,99E-03**
P80723	Brain acid soluble protein 1	1,21E+00	5,38E-01	3,46E+00	**2,16E-03**
P27348	14-3-3 protein theta	9,58E-01	3,96E-01	3,00E+00	**4,39E-03**
Q9BQE5	Apolipoprotein L2	1,64E+00	4,92E-02	2,95E+00	**2,05E-03**
P19971	Thymidine phosphorylase	9,97E-01	7,64E-01	2,79E+00	**4,49E-02**
Q14974	Importin subunit beta-1	9,77E-01	3,78E-01	2,39E+00	**2,39E-02**
P02786	Transferrin receptor protein 1	1,14E+00	7,66E-01	2,20E+00	**4,70E-04**
P08107	Heat shock 70 kDa protein 1A/1B	1,19E+00	4,09E-01	1,93E+00	**1,61E-02**
P20700	Lamin-B1	1,34E+00	4,04E-01	1,85E+00	**3,84E-02**
P34931	Heat shock 70 kDa protein 1-like	1,16E+00	5,18E-01	1,55E+00	**4,28E-02**
Q9BZQ8	Protein Niban	1,14E+00	3,16E-01	1,54E+00	**6,54E-03**
P07339	Cathepsin D	1,68E+00	7,57E-01	6,26E-01	**3,15E-02**
P22897	Macrophage mannose receptor 1	9,76E-01	3,61E-01	6,31E-01	**1,62E-02**
P17900	Ganglioside GM2 activator	1,40E+00	1,85E-01	5,80E-01	**1,61E-02**
Q9UBR2	Cathepsin Z	1,30E+00	**1,23E-02**	5,64E-01	**2,42E-03**

*HLA serotypes originate from the same gene and share common peptides. The serotype attributed to the identification may therefore not be accurate. Red and blue coloured numbers represent higher and lower fold change of proteins compared to iDCs respectively. Statistically significant *p*-values are given in bold.

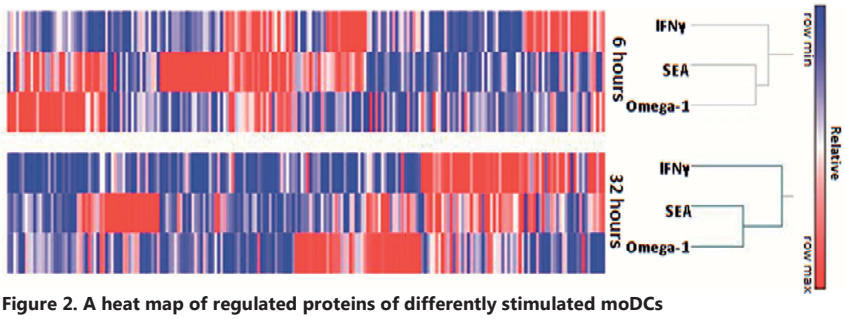

Figure 2. A heat map of regulated proteins of differently stimulated moDCs
Monocyte-derived DCs were stimulated as described in legend of Figure 1, and protein expression was analyzed by Gene E based on the fold change of proteins relative to LPS at 6 and 32 h. Colour indicates directionality of the change in protein expression (red=increase, blue= decrease).

cathepsins, that play a role in antigen processing, and Ganglioside GM2 activator (GM2A) that mediates presentation of lipids [22, 26, 27].

Effects of polarizing stimuli on the human DC proteome

Based on analysis of fold changes of proteins in the different polarizing conditions, compared to LPS, there was a hierarchical clustering based on time (Figure 2). This reflects the differential expression of proteins at 6 h and 32 h after initiation of polarization. The heat map showed that, at each time point, proteins expressed in DCs stimulated with the SEA and ω-1 clustered together, indicating distinct proteome profiles in pro-Th1 *versus* pro-Th2 DCs.

Table 2. Differentially expressed proteins in pro-Th1 and pro-Th2 DCs versus LPS-DCs

Accession	Protein	IFN-γ		SEA		Omega-1	
		Fold	*p*-value	Fold	*p*-value	Fold	*p*-value
IFN-γ-modulated, 6 hours							
P07900	Heat shock protein HSP 90-alpha	2,42E+00	**2,07E-02**	2,98E+00	**1,90E-02**	2,42E+00	1,39E-01
P23381	Tryptophan--tRNA ligase, cytoplasmic	2,13E+00	**3,93E-02**	1,20E+00	4,27E-01	1,07E+00	6,08E-01
P13639	Elongation factor 2	1,82E+00	**9,45E-03**	1,64E+00	1,17E-01	1,34E+00	3,31E-01
P30508*	HLA class I histocompatibility antigen, Cw-12 alpha chain	1,78E+00	**2,95E-02**	1,61E+00	4,08E-01	1,29E+00	9,68E-01
P09467	Fructose-1.6-bisphosphatase 1	1,69E+00	**2,11E-02**	1,54E+00	7,41E-02	1,53E+00	2,47E-01
Q01813	6-phosphofructokinase type C	1,39E+00	**2,10E-02**	1,13E+00	4,27E-01	1,65E+00	**6,14E-03**
P26038	Moesin	6,57E-01	**3,92E-02**	8,58E-01	1,59E-01	1,12E+00	5,77E-01
P67936	Tropomyosin alpha-4 chain	6,57E-01	**1,92E-02**	8,99E-01	1,79E-01	1,08E+00	3,63E-01
P02545	Prelamin-A/C	6,38E-01	**4,80E-03**	9,50E-01	2,09E-01	1,09E+00	7,34E-01
P16070	CD44 antigen	6,32E-01	**1,06E-02**	1,01E+00	3,96E-01	8,89E-01	2,11E-01
P10599	Thioredoxin	5,17E-01	**1,59E-02**	2,31E+00	3,27E-01	1,10E+00	6,85E-02
IFN-γ- modulated, 32 hours							
P09769	Tyrosine-protein kinase Fgr	6,47E-01	**2,73E-02**	6,80E-01	**9,46E-03**	9,47E-01	3,98E-01
P62937	Peptidyl-prolyl cis-trans isomerase A	5,88E-01	**2,87E-04**	9,94E-01	2,85E-01	9,75E-01	3,76E-01
P04908	Histone H2A type 1-B/E	5,77E-01	**1,94E-02**	2,38E+00	4,39E-01	3,71E+00	5,85E-01
P40926	Malate dehydrogenase. mitochondrial	5,53E-01	**4,74E-03**	1,07E+00	1,55E-01	1,31E+00	2,00E-01
SEA- modulated, 6 hours							
P62937	Peptidyl-prolyl cis-trans isomerase A	4,02E+00	4,45E-01	1,13E+01	**1,18E-02**	1,62E+00	5,41E-01
Q9BZQ8**	Protein Niban	1,10E+00	8,53E-01	9,78E+00	**4,42E-06**	1,03E+00	8,94E-01
P14625	Endoplasmin	1,47E+00	5,77E-01	4,14E+00	**3,95E-02**	2,31E+00	8,85E-01
P60842	Eukaryotic initiation factor 4A-I	1,83E+00	3,18E-01	3,21E+00	**4,20E-02**	1,17E+00	4,70E-01
P07900	Heat shock protein HSP 90-alpha	2,42E+00	**2,07E-02**	2,98E+00	**1,90E-02**	2,42E+00	1,39E-01
Q16658	Fascin	1,15E+00	9,19E-01	1,74E+00	**4,10E-02**	1,40E+00	3,18E-01
SEA- modulated, 32 hours							
P05387	60S acidic ribosomal protein P2	1,68E+00	1,75E-01	2,27E+00	**6,25E-03**	4,63E+00	**1,30E-02**
Q9BZQ8**	Protein Niban	1,19E+00	1,96E-01	2,20E+00	**1,10E-02**	1,20E+00	7,31E-01
Q99536	Synaptic vesicle membrane protein VAT-1 homolog	1,29E+00	2,04E-01	1,59E+00	**2,77E-02**	1,53E+00	**1,62E-02**
P09769	Tyrosine-protein kinase Fgr	6,47E-01	**2,73E-02**	6,80E-01	**9,46E-03**	9,47E-01	3,98E-01
P16070	CD44 antigen	1,47E+00	8,09E-01	6,25E-01	**2,34E-02**	4,71E-01	**1,92E-03**
P23381	Tryptophan--tRNA ligase, cytoplasmic	1,45E+00	3,41E-01	6,01E-01	**4,24E-03**	9,21E-01	1,88E-01
P02786	Transferrin receptor protein 1	7,54E-01	5,10E-02	5,65E-01	**1,65E-03**	4,86E-01	**1,54E-03**
P30464*	HLA class I histocompatibility antigen, B-15 alpha chain	1,27E+00	7,93E-01	4,52E-01	**3,34E-03**	3,99E-01	**1,64E-03**

Omega-1- modulated, 6 hours							
P30048	Thioredoxin-dependent peroxide reductase, mitochondrial	7,06E+00	1,43E-01	2,56E+00	6,36E-01	4,03E+00	**3,59E-02**
P05388	60S acidic ribosomal protein P0	1,47E+00	5,70E-02	1,31E+00	6,37E-01	1,86E+00	**2,05E-02**
P30041	Peroxiredoxin-6	1,33E+00	6,30E-01	1,44E+00	3,34E-01	1,77E+00	**2,00E-02**
Q01813	6-phosphofructokinase type C	1,39E+00	**2,10E-02**	1,13E+00	4,27E-01	1,65E+00	**6,14E-03**
P61158	Actin-related protein 3	1,47E+00	4,97E-01	2,11E+00	6,71E-01	1,61E+00	**3,78E-02**
Omega-1- modulated, 32 hours							
P05387	60S acidic ribosomal protein P2	1,68E+00	1,75E-01	2,27E+00	**6,25E-03**	4,63E+00	**1,30E-02**
P27824	Calnexin	1,32E+00	9,32E-01	1,76E+00	5,05E-01	2,64E+00	**4,73E-02**
P55084	Trifunctional enzyme subunit beta, mitochondrial	1,72E+00	1,44E-01	1,48E+00	1,34E-01	2,52E+00	**4,52E-02**
P63104	14-3-3 protein zeta/delta	1,60E+00	5,54E-01	1,51E+00	1,83E-01	2,33E+00	**3,52E-02**
P50502	Hsc70-interacting protein	1,29E+00	4,79E-01	1,45E+00	5,66E-02	2,05E+00	**2,43E-02**
P30041	Peroxiredoxin-6	9,44E-01	3,21E-01	1,46E+00	3,19E-01	2,02E+00	**1,97E-02**
Q99536	Synaptic vesicle membrane protein VAT-1 homolog	1,29E+00	2,04E-01	1,59E+00	**2,77E-02**	1,53E+00	**1,62E-02**
P17900	Ganglioside GM2 activator	1,04E+00	2,04E-01	1,26E+00	6,78E-01	6,54E-01	**2,57E-02**
P30508	HLA class I histocompatibility antigen, Cw-12 alpha chain	1,02E+00	2,89E-01	1,01E+00	5,45E-02	6,32E-01	**1,19E-02**
P29966	Myristoylated alanine-rich C-kinase substrate	1,19E+00	7,78E-01	7,32E-01	6,00E-02	5,84E-01	**1,46E-02**
P04179	Superoxide dismutase [Mn]. mitochondrial	1,30E+00	8,49E-01	1,24E+00	3,72E-01	5,21E-01	**6,19E-03**
P02786	Transferrin receptor protein 1	7,54E-01	5,10E-02	5,65E-01	**1,65E-03**	4,86E-01	**1,54E-03**
P16070	CD44 antigen	1,47E+00	8,09E-01	6,25E-01	**2,34E-02**	4,71E-01	**1,92E-03**
P30504*	HLA class I histocompatibility antigen, Cw-4 alpha chain	7,25E-01	9,92E-02	1,88E+00	2,10E-01	4,66E-01	**1,91E-02**
P30464*	HLA class I histocompatibility antigen, B-15 alpha chain	1,27E+00	7,93E-01	4,52E-01	**3,34E-03**	3,99E-01	**1,64E-03**

*HLA serotypes originate from the same gene and share common peptides. The serotype attributed to the identification may therefore not be accurate. **The signal attributed to the VLTSEDEYNLLSDR peptide in NIBAN is likely coming from $^{13}C_1$-peak of the YCLQLYDETYER peptide from SEA-derived protein IL-4-inducing protein (IPSE). Protein Niban was removed from further analysis. Red and blue coloured numbers represent higher and lower fold change of proteins compared to LPS-DCs respectively. Statistically significant *p*-value of protein change indicated by bold printed *p*-values.

The LPS-IFN-γ stimulated DCs differentially expressed eleven proteins after 6h of stimulation compared to stimulation with LPS alone (Table 2). Five proteins were downregulated, of which three were members of the cytoskeleton. The proteins most strongly upregulated were Heat Shock Protein HSP 90-alpha (HSP90AA1), which mediates inflammatory responses, and cytoplasmic tryptophan-tRNA ligase (WARS), also known as Interferon-induced protein 53 (p53). After 32 h, four proteins were downregulated (Table 2), including a tyrosine-protein kinase involved in regulation of immune responses (FGR), and Peptidyl-prolyl cis-trans isomerase A (PPIA), which plays an important role in protein folding, trafficking, and immune cell activation [28].

Following 6 h of stimulation with Th2-inducing SEA, five proteins were upregulated compared to stimulation with LPS alone (Table 2). SEA induced upregulation of PPIA which is involved in various cellular functions including protein folding, T cell activation and differentiation [28]. SEA also increased expression of Eukaryotic initiation factor 4A-I, which played a role in the initiation of the translation process. The expression of both chaperones of HSP90, namely Endoplasmin (HSP90B1) and HSP90AA1 were increased with SEA stimulation. Interestingly, HSP90 is a protein that is important for type I interferon production [29], which was recently found to be a key transcriptional signature of murine skin DCs and that enable them to drive Th2 responses in response to helminth antigens [30]. However, given that HSP90AA1 was also observed to be

upregulated by IFN-γ and that we could not find a clear type I interferon signature in the SEA or ω-1 stimulated DCs, makes it unlikely that this pathway is of importance for Th2 induction by SEA or ω-1-stimulated DCs. The fifth upregulated protein by SEA was seen at 6 h after SEA stimulation and was identified as Fascin, known to be involved in cell motility, migration and regulation of the cytoskeleton. After 32 h, SEA promoted differential expression of seven proteins (Table 2). Among those, five proteins were downregulated, including WARS which was upregulated by IFN-γ (at 6h), a MHC class I protein complex HLA-B and CD44 which are involved in antigen presentation and T cell activation, respectively [31]. The protein most strongly upregulated at 32 h of SEA stimulation was 60S acidic ribosomal protein P2 (RPLP2), which plays an important role in the elongation step of protein synthesis.

Omega-1 induced upregulation of five proteins after 6 h, and seven proteins after 32 h (Table 2), most of which were ribosomal proteins, chaperones or enzymes. Among those, several proteins were highly upregulated, including mitochondrial Thioredoxin-dependent peroxide reductase (6 h), a protein involved in redox regulation of the cell, RPLP2 (32 h), and the chaperone Calnexin (32 h). After 32 h of ω-1 stimulation, eight proteins were downregulated. In particular, ω-1 strongly decreased expression of HLA-B, HLA-C and CD44, as well as MARCS.

Analysis of proteins exclusive to the Th2-inducing proteome

The identification of proteins uniquely associated with the Th2-inducing DC proteome could provide valuable leads for understanding how DCs initiate Th2 responses. We therefore analyzed proteins affected by stimulation with SEA as well as ω-1, by looking at protein expression dynamics and individual donor responses. As can be appreciated from Table 2, ω-1 and SEA did not share proteins that indicate Th2 commitment after 6h of stimulation. After 32h, however, they shared five differentially expressed proteins. Among those five, Transferrin receptor protein 1 is seemingly downregulated by omega-1 and SEA, but also by IFN-γ (ρ=0.051), suggesting that this may not be a Th2-exclusive protein.

Analysis of protein expression dynamics of the four remaining Th2-associated proteins showed that RPLP2 was strongly upregulated by 32h of stimulation with SEA and omega-1 in at least eight out of nine donors (Figure 3A). Synaptic vesicle membrane protein VAT-1 homolog (VAT1) was upregulated by SEA and omega-1 in at least seven donors after 32h of stimulation (Figure 3B), but was also mildly increased by IFN-γ stimulation in the majority of donors. CD44 was significantly downregulated by SEA in seven donors, and by ω-1 in nine donors (Figure 3C). Lastly, LPS-induced upregulation of HLA-B was inhibited by SEA and ω-1 in eight donors (Figure 3D). These findings suggest that in particular upregulation of RPLP2, and downregulation of CD44 and HLA-B, are unique characteristics of pro-Th2 DCs.

DISCUSSION

Over the past decade, studies on the proteome of matured or polarized DCs relied on label- and gel-based techniques. Such approaches do not allow for high-throughput analysis of many different conditions or biological replicates, which might explain why only few proteins were found in common between different reports [10, 11, 14, 15, 32]. Here, we used ion traps for tandem mass spectrometry and LC-FTICRMS for label- and gel-free quantitation. The method is an AMTs-based analysis [17, 33], with the peptide identification being done in parallel with the FTICR measurement in the same instrument cluster. The bridging of peptide identification across LC-MS runs is performed through chromatographic alignment [19, 34]. This method had previously been used

for the analysis of the proteome from human plasma and the cells from a bacterium, *Deinococcus radiodurans* [16, 19]. This approach allowed us to analyze the most abundant proteins and to generate an overview of global proteome changes of LPS-matured and pro-Th1 versus pro-Th2 DCs from nine different human donors.

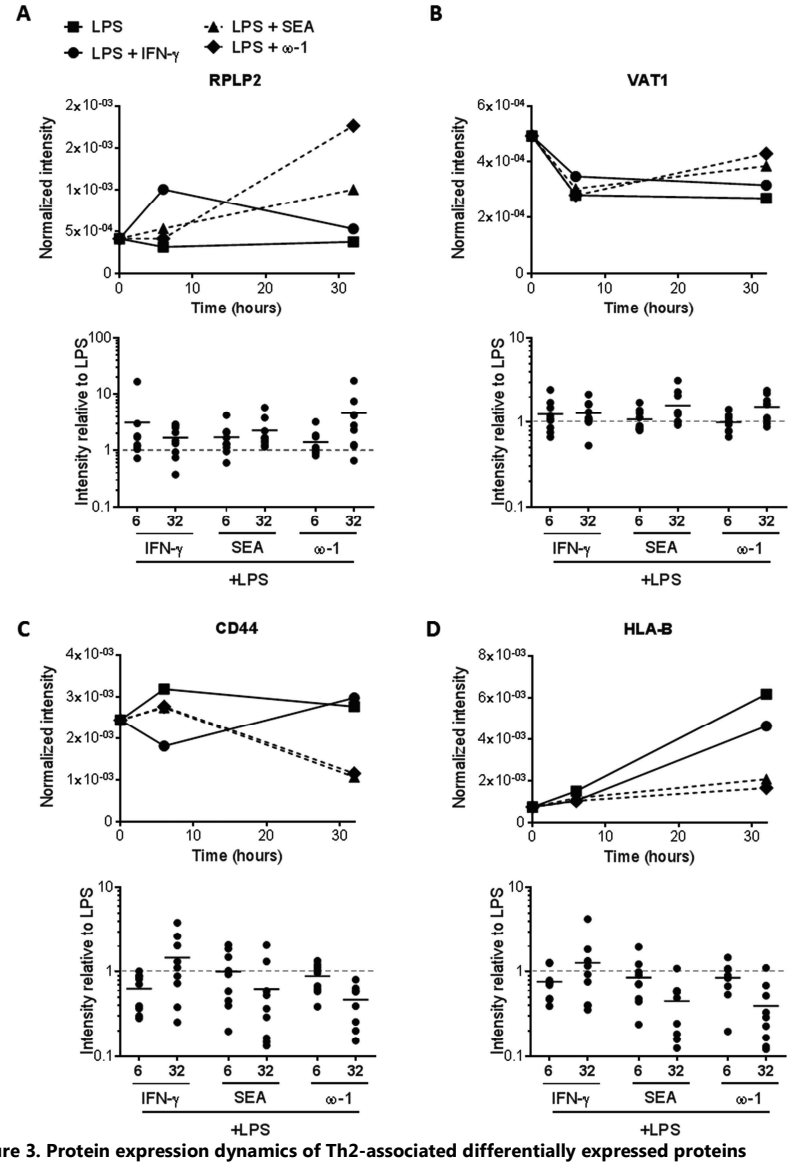

Figure 3. Protein expression dynamics of Th2-associated differentially expressed proteins
Monocyte-derived DCs were stimulated as described for the legend of Figure 1. Protein expression was analyzed by LC-FTICRMS. Differentially expressed proteins shared between 32 h of stimulation of with ω-1 and SEA are shown. The top panel of each figure shows the protein expression dynamics, the bottom panel shows the normalized intensity relative to LPS, which was set to 1 at 6 h and at 32 h (dashed line). (A) 60S acidic ribosomal protein P2. (B) Synaptic vesicle membrane protein VAT-1 homolog. (C) CD44 antigen. (D) HLA-B.

As expected, LPS-induced maturation resulted in a pronounced effect on the DC proteome. After 6 h of maturation, proteins involved in intracellular transport and cell communication were upregulated, and cytoskeletal proteins were either up- or downregulated. These processes may reflect that the DCs are preparing for migration, which requires profound alterations in cell morphology and motility [35]. The strongest effect on the DC proteome was observed after 32 h of LPS-induced maturation, when many proteins were upregulated at least 3-fold. Among the proteins most strongly induced was mitochondrial Superoxide dismutase (SODM). Indeed, DCs are known to upregulate reactive oxygen species in response to stimulation with LPS [36, 37], and subsequent upregulation of superoxide dismutases has also been reported [38]. In addition, stimulation with LPS induced Fascin, an actin cross-linking protein that plays a critical role in migration of mature DCs into lymph nodes. Specifically, actin bundling by Fascin was shown to promote membrane protrusions and mediates disassembly of podosomes, which are specialized structures for cell-matrix adhesion [39]. A second actin cross-linking protein, MARCS, was also profoundly induced, in line with a previous report [40]. The other two proteins most strongly affected by LPS stimulation were MHC class I molecule HLA-B, involved in antigen presentation, and TRAF1, an adapter molecule that regulates activation of NF-κB and JNK. Indeed, NF-κB activation was previously shown to be required for DC maturation [41]. The proteins downregulated after 32 h of LPS stimulation were involved in antigen uptake, processing and presentation of lipids. Together, these findings reflect that after 32 h of stimulation, LPS-DCs have become specialized for entering lymph nodes and presenting antigen to naive T cells, which identifies and validates the FTICR-ion trap cluster as an appropriate method to for high-throughput quantitative analysis of dendritic cell lysates.

Importantly, we find many differentially expressed proteins in common with a proteomics study by Ferreira *et al.* [14], which further validates our method. In our and their study, maturation reduces expression of cathepsins and GM2A, and increases expression of Apolipoprotein L2, Fascin, Proteasome activator complex subunit 2, and SODM. Furthermore, in line with another report [15], we observe an increase in Heath shock protein (Hsp) expression. Unique to our study, the FTICR method allowed us to perform statistical analysis on protein expression data from nine biological replicates. In addition, two time points were included, which provides information about protein expression dynamics. Indeed we were able to show that the detected proteins were differently regulated at earlier compared to the later time points after DC maturation. Our study therefore strengthens and expands previous reports on maturation of human DCs.

Using the cytokine IFN-γ, we polarized LPS-DCs for Th1 skewing, and observed that pro-Th1 DCs differentially expressed cytoskeletal proteins and proteins involved in inflammatory processes after 6 h of stimulation, compared to LPS-DCs. Among those proteins, HSP90AA1 and cytoplasmic tryptophan-tRNA ligase (WARS) were most strongly upregulated. Indeed, under inflammatory conditions, heat shock proteins (HSPs) can act as chaperones to facilitate antigen presentation and enhance the immune response [42]. In line with our results, Ferreira *et al.* also described upregulation of WARS in DCs following LPS + IFN-γ treatment [14]. WARS is an ubiquitous enzyme responsible for the association of tryptophan with its specific tRNA, resulting in Trp-tRNA complex used for protein synthesis. Therefore, IFN-γ seems to affect tryptophan metabolism in dendritic cells, which is also in line with the report that WARS mRNA expression in peripheral blood mononuclear cells is dependent on IFN-γ [43]. However, the exact role of WARS in DC-mediated T cell activation remains to be determined. After 32 h of IFN-γ stimulation, the effect on the DC proteome was less pronounced, as only 4 proteins were downregulated, including PPIA involved in

immune regulation and activation [28] and FGR, a tyrosine-protein kinase involved in cell migration regulating cytoskeletal reorganization [44]. Together these findings may suggest that IFN-γ treatment induces strong effects early after treatment, reminiscent of accelerated maturation, whereas at later time point, the changes reflect a less active state.

Interestingly, in contrast to 32 h of treatment with IFN-γ, short-term (6 h) stimulation of DCs with Th2-inducing SEA promoted strong expression of PPIA , also known as Cyclophilin A (CyA), which is the primary binding protein of Cyclosporin A, an immunosuppressive drug. The cyclophilin and cyclosporine complex, leads to anti-inflammatory responses [28, 45]. Increased levels of cyclophilin A have been reported following oxidative stress response [28] as well as during fibrosis [46]. Interestingly, a recent study found that CyA is highly expressed in both worm and SEA of *S. japonicum* and showed that injection of schistosome CyA facilited Th2 responses [47]. As both SEA, which is an antigenic mix, as well as ω-1, a pure SEA-derived protein, induce CyA, it is unlikely that in our model CyA is a parasite-derived protein. Moreover, the downregulation of CyA in IFN-γ conditioned DCs would also suggest that this is a molecule expressed by DCs, that is involved in DC polarization. The protein FGR was also downregulated after 32 h SEA treatment similar to that seen after IFN-γ stimulation.

The most profound effect of Th2-inducing stimuli was observed after 32h of stimulation, when SEA and ω-1 both strongly increased expression of ribosomal protein RPLP2. The ribosomal proteins are known for playing an important role in ribosome assembly and protein translation, suggesting that SEA and ω-1 are affecting these processes. However, they can also have extra-ribosomal functions. For instance, stress responses can be associated with increased levels of ribosomal proteins that in turn affect immune signaling [48]. Whether or not SEA- and ω-1-induced RPLP2 expression serves extra-ribosomal functions requires further investigation. Another upregulated protein was synaptic vesicle membrane protein VAT-1 homolog, known as negative regulator of mitochondrial fusion, which works in cooperation with mitofusin proteins (MFN1-2) [49]. Decrease in mitochondria fusion will lead to impairment of the oxidative phosporylation (OXPHOS) [50]. This finding suggests that SEA and ω-1 may affect cellular metabolism. Recent studies have indicated that modulation of metabolic pathways within dendritic cells can regulate DC function and the outcome of the immune response [51, 52]. Whether ω-1 and SEA skew responses towards Th2 through changing cellular metabolism, requires further studies. In addition, SEA and ω-1 decreased expression of CD44 and suppressed LPS-induced upregulation of HLA-B. Interestingly, CD44 expression by DCs was shown to promote CD4 T cell proliferation [31]. Together, these findings may suggest that Th2-inducing conditions interfere with efficient antigen presentation to T cells. It has been suggested that T cells are polarized towards Th2 if the interaction between DCs and T cells is weak [53-55]. In line with this, it was demonstrated that ω-1 reduces the capacity of bone marrow-derived DCs to form T cell-DC conjugates [8]. Also our own preliminary data point towards a reduced ability of SEA and ω-1-stimulated DCs to expand $CD4^+$ T cells, compared to Th1 polarizing DCs (data not shown).

In conclusion, our work has identified the FTICR-ion trap cluster as an appropriate method for quantitative high-throughput analysis of cell lysates. Our data on DC polarization suggest that pro-Th1 DCs undergo accelerated maturation compared to LPS-DCs, and indicate that pro-Th2 DCs may affect cellular metabolism and decrease expression of proteins involved in antigen processing and presentation. Future research should therefore focus on studying the contribution of metabolic pathways, TCR signaling, and the possible relation between the two, to further dissect the mechanisms of helminth-induced T helper 2 polarization via dendritic cells. Moreover, this

proteomic approach will also be a valuable tool in future studies to assess in unbiased manner the proteomes DCs that favor induction of Th17 and Tregs, that together with the current work could function as important resource for DC biologists. Finally, such investigations will not only improve our fundamental understanding of DC biology, but will also help in the identification of proteins or pathways that can targeted in DCs to shape their Th cell-polarizing characteristics. This could be particularly important for the rational design of DC-based immunotherapies as well as for development and/or improving efficacy of vaccines against parasitic as well as other infections.

ACKNOWLEDGEMENTS

This project was supported by the EU (HEALTH-F3-2009-241642). The authors thank The Indonesian Directorate General of Higher Education (DIKTI)-Leiden University for providing a PhD scholarship to Maria M. M. Kaisar.

REFERENCES

1. Steinman, R.M. and Z.A. Cohn, *Identification of a novel cell type in peripheral lymphoid organs of mice. I. Morphology, quantitation, tissue distribution.* J Exp Med, 1973. **137**(5): p. 1142-62.
2. Kapsenberg, M.L., *Dendritic-cell control of pathogen-driven T-cell polarization.* Nat Rev Immunol, 2003. **3**(12): p. 984-93.
3. Tato, C.M. and J.J. O'Shea, *Immunology: what does it mean to be just 17?* Nature, 2006. **441**(7090): p. 166-8.
4. Zelante, T., et al., *IL-17/Th17 in anti-fungal immunity: what's new?* Eur J Immunol, 2009. **39**(3): p. 645-8.
5. Hussaarts, L., M. Yazdanbakhsh, and B. Guigas, *Priming dendritic cells for th2 polarization: lessons learned from helminths and implications for metabolic disorders.* Front Immunol, 2014. **5**: p. 499.
6. Mathieson, W. and R.A. Wilson, *A comparative proteomic study of the undeveloped and developed Schistosoma mansoni egg and its contents: the miracidium, hatch fluid and secretions.* Int J Parasitol, 2010. **40**(5): p. 617-28.
7. Everts, B., et al., *Omega-1, a glycoprotein secreted by Schistosoma mansoni eggs, drives Th2 responses.* J Exp Med, 2009. **206**(8): p. 1673-80.
8. Steinfelder, S., et al., *The major component in schistosome eggs responsible for conditioning dendritic cells for Th2 polarization is a T2 ribonuclease (omega-1).* J Exp Med, 2009. **206**(8): p. 1681-90.
9. Everts, B., et al., *Schistosome-derived omega-1 drives Th2 polarization by suppressing protein synthesis following internalization by the mannose receptor.* J Exp Med, 2012. **209**(10): p. 1753-67, s1.
10. Pereira, S.R., et al., *Changes in the proteomic profile during differentiation and maturation of human monocyte-derived dendritic cells stimulated with granulocyte macrophage colony stimulating factor/interleukin-4 and lipopolysaccharide.* Proteomics, 2005. **5**(5): p. 1186-98.
11. Gundacker, N.C., et al., *Cytoplasmic proteome and secretome profiles of differently stimulated human dendritic cells.* J Proteome Res, 2009. **8**(6): p. 2799-811.
12. Ferret-Bernard, S., R.S. Curwen, and A.P. Mountford, *Proteomic profiling reveals that Th2-inducing dendritic cells stimulated with helminth antigens have a 'limited maturation' phenotype.* Proteomics, 2008. **8**(5): p. 980-93.
13. Ferret-Bernard, S., et al., *Plasma membrane proteomes of differentially matured dendritic cells identified by LC-MS/MS combined with iTRAQ labelling.* J Proteomics, 2012. **75**(3): p. 938-48.
14. Ferreira, G.B., et al., *Protein-induced changes during the maturation process of human dendritic cells: A 2-D DIGE approach.* Proteomics Clin Appl, 2008. **2**(9): p. 1349-60.
15. Richards, J., et al., *Integrated genomic and proteomic analysis of signaling pathways in dendritic cell differentiation and maturation.* Ann N Y Acad Sci, 2002. **975**: p. 91-100.
16. Johansson, A., et al., *Identification of genetic variants influencing the human plasma proteome.* Proc Natl Acad Sci U S A, 2013. **110**(12): p. 4673-8.
17. Palmblad, M., et al., *A novel mass spectrometry cluster for high-throughput quantitative proteomics.* J Am Soc Mass Spectrom, 2010. **21**(6): p. 1002-11.
18. Hussaarts, L., et al., *Rapamycin and omega-1: mTOR-dependent and -independent Th2 skewing by human dendritic cells.* Immunol Cell Biol, 2013. **91**(7): p. 486-9.
19. Smith, R.D., et al., *An accurate mass tag strategy for quantitative and high-throughput proteome measurements.* Proteomics, 2002. **2**(5): p. 513-23.

20. Wolstencroft, K., et al., *The Taverna workflow suite: designing and executing workflows of Web Services on the desktop, web or in the cloud.* Nucleic Acids Res, 2013. **41**(Web Server issue): p. W557-61.
21. Craig, R. and R.C. Beavis, *TANDEM: matching proteins with tandem mass spectra.* Bioinformatics, 2004. **20**(9): p. 1466-7.
22. Kolter, T. and K. Sandhoff, *Principles of lysosomal membrane digestion: stimulation of sphingolipid degradation by sphingolipid activator proteins and anionic lysosomal lipids.* Annu Rev Cell Dev Biol, 2005. **21**: p. 81-103.
23. Palmblad, M., et al., *Chromatographic alignment of LC-MS and LC-MS/MS datasets by genetic algorithm feature extraction.* J Am Soc Mass Spectrom, 2007. **18**(10): p. 1835-43.
24. Keller, A., et al., *Empirical statistical model to estimate the accuracy of peptide identifications made by MS/MS and database search.* Anal Chem, 2002. **74**(20): p. 5383-92.
25. Lee, S.Y. and Y. Choi, *TRAF1 and its biological functions.* Adv Exp Med Biol, 2007. **597**: p. 25-31.
26. Katunuma, N., et al., *Insights into the roles of cathepsins in antigen processing and presentation revealed by specific inhibitors.* Biol Chem, 2003. **384**(6): p. 883-90.
27. Martinez-Pomares, L., *The mannose receptor.* J Leukoc Biol, 2012. **92**(6): p. 1177-86.
28. Nigro, P., G. Pompilio, and M.C. Capogrossi, *Cyclophilin A: a key player for human disease.* Cell Death Dis, 2013. **4**: p. e888.
29. Saito, K., et al., *Heat shock protein 90 associates with Toll-like receptors 7/9 and mediates self-nucleic acid recognition in SLE.* Eur J Immunol, 2015. **45**(7): p. 2028-41.
30. Connor, L.M., et al., *Th2 responses are primed by skin dendritic cells with distinct transcriptional profiles.* J Exp Med, 2017. **214**(1): p. 125-142.
31. Termeer, C., et al., *Targeting dendritic cells with CD44 monoclonal antibodies selectively inhibits the proliferation of naive CD4+ T-helper cells by induction of FAS-independent T-cell apoptosis.* Immunology, 2003. **109**(1): p. 32-40.
32. Ferreira, G.B., C. Mathieu, and L. Overbergh, *Understanding dendritic cell biology and its role in immunological disorders through proteomic profiling.* Proteomics Clin Appl, 2010. **4**(2): p. 190-203.
33. Strittmatter, E.F., et al., *Proteome analyses using accurate mass and elution time peptide tags with capillary LC time-of-flight mass spectrometry.* J Am Soc Mass Spectrom, 2003. **14**(9): p. 980-91.
34. Jaitly, N., et al., *Robust algorithm for alignment of liquid chromatography-mass spectrometry analyses in an accurate mass and time tag data analysis pipeline.* Anal Chem, 2006. **78**(21): p. 7397-409.
35. Alvarez, D., E.H. Vollmann, and U.H. von Andrian, *Mechanisms and consequences of dendritic cell migration.* Immunity, 2008. **29**(3): p. 325-42.
36. Matsue, H., et al., *Generation and function of reactive oxygen species in dendritic cells during antigen presentation.* J Immunol, 2003. **171**(6): p. 3010-8.
37. Yamada, H., et al., *LPS-induced ROS generation and changes in glutathione level and their relation to the maturation of human monocyte-derived dendritic cells.* Life Sci, 2006. **78**(9): p. 926-33.
38. Rivollier, A., et al., *High expression of antioxidant proteins in dendritic cells: possible implications in atherosclerosis.* Mol Cell Proteomics, 2006. **5**(4): p. 726-36.
39. Yamakita, Y., et al., *Fascin1 promotes cell migration of mature dendritic cells.* J Immunol, 2011. **186**(5): p. 2850-9.
40. Buhligen, J., et al., *Lysophosphatidylcholine-mediated functional inactivation of syndecan-4 results in decreased adhesion and motility of dendritic cells.* J Cell Physiol, 2010. **225**(3): p. 905-14.
41. Rescigno, M., et al., *Dendritic cell survival and maturation are regulated by different signaling pathways.* J Exp Med, 1998. **188**(11): p. 2175-80.
42. Srivastava, P., *Roles of heat-shock proteins in innate and adaptive immunity.* Nat Rev Immunol, 2002. **2**(3): p. 185-94.
43. Boasso, A., et al., *Regulation of indoleamine 2,3-dioxygenase and tryptophanyl-tRNA-synthetase by CTLA-4-Fc in human CD4+ T cells.* Blood, 2005. **105**(4): p. 1574-81.
44. Suen, P.W., et al., *Impaired integrin-mediated signal transduction, altered cytoskeletal structure and reduced motility in Hck/Fgr deficient macrophages.* J Cell Sci, 1999. **112 (Pt 22)**: p. 4067-78.
45. Obchoei, S., et al., *Cyclophilin A: potential functions and therapeutic target for human cancer.* Med Sci Monit, 2009. **15**(11): p. Ra221-32.
46. Yuan, Y., et al., *Proteomic identification of cyclophilin A as a potential biomarker and therapeutic target in oral submucous fibrosis.* Oncotarget, 2016.
47. Li, J., et al., *Cyclophilin A from Schistosoma japonicum promotes a Th2 response in mice.* Parasit Vectors, 2013. **6**: p. 330.
48. Zhou, X., et al., *Ribosomal proteins: functions beyond the ribosome.* J Mol Cell Biol, 2015. **7**(2): p. 92-104.
49. Eura, Y., et al., *Identification of a novel protein that regulates mitochondrial fusion by modulating mitofusin (Mfn) protein function.* J Cell Sci, 2006. **119**(Pt 23): p. 4913-25.

50. Mishra, P. and D.C. Chan, *Metabolic regulation of mitochondrial dynamics*. J Cell Biol, 2016. **212**(4): p. 379-87.
51. Pearce, E.J. and B. Everts, *Dendritic cell metabolism*. Nat Rev Immunol, 2015. **15**(1): p. 18-29.
52. Pearce, E.L. and E.J. Pearce, *Metabolic pathways in immune cell activation and quiescence*. Immunity, 2013. **38**(4): p. 633-43.
53. Constant, S., et al., *Extent of T cell receptor ligation can determine the functional differentiation of naive CD4+ T cells*. J Exp Med, 1995. **182**(5): p. 1591-6.
54. Hosken, N.A., et al., *The effect of antigen dose on CD4+ T helper cell phenotype development in a T cell receptor-alpha beta-transgenic model*. J Exp Med, 1995. **182**(5): p. 1579-84.
55. van Panhuys, N., F. Klauschen, and R.N. Germain, *T-cell-receptor-dependent signal intensity dominantly controls CD4(+) T cell polarization In Vivo*. Immunity, 2014. **41**(1): p. 63-74.